



CHORUS

This is the accepted manuscript made available via CHORUS. The article has been published as:

Fermi surfaces and quantum oscillations in the underdoped high- T_c superconductors $\text{YBa}_{2}\text{Cu}_{3}\text{O}_{6.5}$ and $\text{YBa}_{2}\text{Cu}_{4}\text{O}_{8}$

Hyungju Oh, Hyoung Joon Choi, Steven G. Louie, and Marvin L. Cohen

Phys. Rev. B **84**, 014518 — Published 27 July 2011

DOI: [10.1103/PhysRevB.84.014518](https://doi.org/10.1103/PhysRevB.84.014518)

Fermi surfaces and quantum oscillations in underdoped high- T_c superconductors $\text{YBa}_2\text{Cu}_3\text{O}_{6.5}$ and $\text{YBa}_2\text{Cu}_4\text{O}_8$

Hyungju Oh,¹ Hyoung Joon Choi,^{1,*} Steven G. Louie,^{2,3} and Marvin L. Cohen^{2,3}

¹*Department of Physics and IPAP, Yonsei University, Seoul 120-749, Korea*

²*Department of Physics, University of California, Berkeley, California 94720, USA*

³*Materials Sciences Division, Lawrence Berkeley National Laboratory, Berkeley, California 94720, USA*

(Dated: June 2, 2011)

We study underdoped high- T_c superconductors $\text{YBa}_2\text{Cu}_3\text{O}_{6.5}$ and $\text{YBa}_2\text{Cu}_4\text{O}_8$ using first-principles pseudopotential methods with additional Coulomb interactions at the Cu atoms, and obtain Fermi-surface pocket areas in close agreement with measured Shubnikov-de Haas and de Haas-van Alphen oscillations. With antiferromagnetic order in CuO_2 planes, stable in the calculations, small hole pockets are formed near the so-called Fermi-arc positions in the Brillouin zone which reproduce the low-frequency oscillations. A large electron pocket, necessary for the negative Hall coefficient, is also formed in $\text{YBa}_2\text{Cu}_3\text{O}_{6.5}$, giving rise to the high-frequency oscillations as well. Effective masses and specific heats are also calculated. Our results highlight the important role of magnetic order in the electronic structure of underdoped high- T_c superconductors.

PACS numbers: 71.18.+y, 74.25.Jb, 74.72.-h, 74.25.Ha

The normal-state electronic structures of the underdoped high- T_c superconductors have been studied for more than twenty years, but the Fermi-surface (FS) topology is still only partially understood¹⁻¹⁴. An important observation is the disconnected FSs^{1,2}, namely Fermi arcs, observed in angle-resolved photoemission spectroscopy (ARPES), which initiated intense investigations about whether the FSs are really disconnected arcs or closed pockets of which one side is hardly visible in ARPES. Recently, in contrast to having Fermi arcs, de Haas-van Alphen (dHvA) oscillations in the magnetization and Shubnikov-de Haas (SdH) oscillations in the resistance³⁻⁷ observed in ortho-II $\text{YBa}_2\text{Cu}_3\text{O}_{6.5}$ and $\text{YBa}_2\text{Cu}_4\text{O}_8$ suggest well-defined close pockets in the FS of underdoped high- T_c cuprates. The measured oscillations for $\text{YBa}_2\text{Cu}_3\text{O}_{6.5}$ are a dominant one at 500 ± 20 T with a satellite at 1650 ± 40 T⁵, and more recently a dominant oscillation at 540 ± 15 T with satellites at 450 ± 15 T, 630 ± 40 T, and 1130 ± 20 T⁶. For $\text{YBa}_2\text{Cu}_4\text{O}_8$, oscillation at 660 ± 15 T is observed⁷.

The measured dHvA and SdH oscillations provide extreme cross-sectional areas of closed FS pockets¹⁸, but they alone are not enough to identify the shapes and locations of the pockets. Thus, a quantitative theoretical calculation of the FS geometry can be useful to determine the FS topology. First-principles calculations based on the density functional theory (DFT) approach have been performed for $\text{YBa}_2\text{Cu}_3\text{O}_{6.5}$ and $\text{YBa}_2\text{Cu}_4\text{O}_8$ ^{8,9}, but the calculated FSs could not explain the oscillation measurements. In contrast to the measurements, reported DFT calculations predict only FS pockets much larger than 500 T, and do not obtain the electron-type carriers implied by the observed negative Hall coefficients¹⁰.

According to model calculations¹¹⁻¹⁷, antiferromagnetic (AFM) order, a d -density wave, or a stripe order may result in small pockets in regions of the FS. Although using DFT, one may examine static magnetic order using spin-density functional theory¹⁹; as yet, no magnetic order has been considered in the reported DFT calculations of $\text{YBa}_2\text{Cu}_3\text{O}_{6.5}$ and $\text{YBa}_2\text{Cu}_4\text{O}_8$.

In this paper, we present, for the first time, first-principles DFT calculations of $\text{YBa}_2\text{Cu}_3\text{O}_{6.5}$ and $\text{YBa}_2\text{Cu}_4\text{O}_8$ with a Coulomb repulsion U at Cu sites which yield FSs consistent with the dHvA and SdH measurements. We show that, with physically reasonable U values, the AFM order in the CuO_2 planes reconstructs the FS and produces pockets with sizes consistent with the measured frequencies. Moreover, the calculated FS of $\text{YBa}_2\text{Cu}_3\text{O}_{6.5}$ has a large electron pocket which explains the observed negative Hall coefficients. In addition, cyclotron effective masses and specific heats are calculated and compared with experiments. Our results support the possible importance of magnetic order in the electronic structures of underdoped high- T_c cuprates.

Our present work is based on *ab-initio* pseudopotential density-functional calculations with pseudo-atomic orbitals to expand the electronic wavefunctions²⁰. Coulomb interaction at Cu d orbitals, parameterized by U and J ²¹, is added to the local (spin) density approximation [L(S)DA+ U]. With experimental atomic structures^{22,23}, we minimize the total energy with respect to the magnetic moments of Cu atoms in the CuO_2 planes and CuO chains to consider the possibility of AFM order. Our results are that $\text{YBa}_2\text{Cu}_3\text{O}_6$ is an AFM insulator (using $U = 8.0$ eV and $J = 1.34$ eV) and $\text{YBa}_2\text{Cu}_3\text{O}_7$ is a non-magnetic metal (using $U = J = 0$).

Using the LDA+ U method with no magnetic order, we obtain the electronic structure for $\text{YBa}_2\text{Cu}_3\text{O}_{6.5}$ (Figs. 1a and 1b), which are in good agreement with previous calculations⁸. The FS has only large hole pockets and open orbits (Fig. 1b); however, this is not in agreement with the observed quantum oscillations.

When magnetic order is considered in the LSDA+ U calculations for $\text{YBa}_2\text{Cu}_3\text{O}_{6.5}$, (π, π) AFM order is stabilized

in the CuO_2 planes, with neighboring Cu magnetic moments pointing in opposite directions, and this drastically changes the electronic structures (Figs. 1c and 1d). With $U = 6.0$ eV and $J = 1.0$ eV, each Cu atom in the CuO_2 plane has 0.48 Bohr magneton (μ_B), while the CuO chains are still non-magnetic. The FS (Fig. 1d) now consists of small hole pockets (α and α' indicating the two largest ones) and a large electron pocket (β). The calculated pocket areas, which are not very sensitive to U and J around the used values, are in good agreement with the experimental observations (Fig. 1f). This shows that the AFM order^{24,25} may be a way to quantitatively explain the measured dHvA and SdH frequencies.

Figure 1d shows that the hole pockets (α and α') are located at $(\pm\frac{\pi}{2}, \pm\frac{\pi}{2})$, close to the positions of the Fermi arcs in the ARPES data^{1,2}. This supports the idea that slow AFM fluctuation²⁶ may form hole pockets near $(\pm\frac{\pi}{2}, \pm\frac{\pi}{2})$, with their shapes possibly modified to form the arcs because of short-range fluctuation^{11,12}.

Figure 1d also shows that the electron pocket (β) is much more anisotropic than the hole pockets (α and α'). This arises because the electron pocket is derived from CuO-chain states moving along the chain and CuO_2 -plane states moving perpendicular to the chain, while the hole pockets come from the CuO_2 plane only. To have an isotropic resistivity as observed in experiments at temperature below 80 K^{3,27}, we find that the electron mean free path for the CuO-chain states should be about one quarter of that for CuO_2 -plane states in the β pocket because of difference in the group velocities. The presence of ordered CuO chains is essential for the metallicity of ortho-II $\text{YBa}_2\text{Cu}_3\text{O}_{6.5}$. With broken CuO chains, we obtain an almost insulating phase for $\text{YBa}_2\text{Cu}_3\text{O}_{6.5}$.

For more detailed comparison, Fig. 2a shows the k_z dependence of FS pocket areas. The three largest extreme areas of hole pockets are 485 and 621 T at $k_z=0$ and 708 T at $k_z=\pi/c$ (Fig. 2a), which overestimate by about 15 % the experimental low frequencies, 450, 540, and 630 T⁶. The largest extreme area of the electron pocket (β) is 1450 T at $k_z=0$ (Fig. 2a), and it underestimates by 12 % the experimental high frequency, 1650 T⁵. If the Fermi level is shifted to higher energy, hole pockets would shrink and the electron pocket would expand (Figs. 2b and 2c). With a Fermi-level shift (ΔE_F) of 4 meV above the charge-neutrality level, the extreme pocket sizes become 441, 564, and 652 T for the holes and 1519 T for the electron, respectively, resulting in closer agreement with experimental results. Since FS pocket areas change slowly with the AFM ordering vector²⁸, our results using the (π, π) AFM order approximate incommensurate cases close to the (π, π) order.

We calculate the cyclotron effective masses (Figs. 2b and 2c) and the electronic contribution to the normal-state specific heat from the LSDA+ U electronic structure of $\text{YBa}_2\text{Cu}_3\text{O}_{6.5}$. The obtained cyclotron effective masses are 1.78 times the free electron mass (m_e) for the α' pocket and 1.88 m_e for the β pocket. These values are smaller than measured values, 1.78 \sim 1.9 m_e for the low frequency and 3.8 m_e for the high frequency³⁻⁵, but they are consistent with experiments in the sense that the effective mass of the low-frequency oscillation (from the α' pocket in our result) is smaller than that of the high-frequency oscillation (from the β pocket in our result). The calculated Sommerfeld coefficient for the normal-state specific heat is 9.28 $\text{mJ}\cdot\text{mol}^{-1}\cdot\text{K}^{-2}$, slightly smaller than the experimental value of 10 $\text{mJ}\cdot\text{mol}^{-1}\cdot\text{K}^{-2}$ ²⁹. The differences between our values and the measured ones may originate from many-body effects.

The presence of the electron pocket in our FS (Fig. 1d) definitely opens a chance of a negative Hall coefficient, but it alone is not sufficient since the total numbers of holes and electrons in our calculation are equal to each other to represent a charge-neutral stoichiometric sample. Since the Hall coefficient is inversely proportional to the net charge of the carriers, a slight imbalance of the two types of carriers would result in a relatively large Hall coefficient. With $\Delta E_F = 4$ meV, as discussed above for the oscillation frequencies, we can obtain a negative Hall coefficient of -25 mm^3C^{-1} at 70 T (Fig. 3a), close to the experimental value of about -30 mm^3C^{-1} ¹⁰.

Figure 3 shows the Hall coefficients obtained by semiclassical transport theory within the relaxation-time approximation, assuming temperature-dependent but field-independent mean free paths (λ) and $\Delta E_F = 4$ meV. At 50 K, we assume isotropic λ 's for holes, which are 40 nm for the α and α' pockets and 10 nm for the other smaller pockets, and anisotropic λ for electrons (β), which are 20 and 80 nm for CuO-chain and CuO_2 -plane states, respectively. At 1.5 K they are increased to ten times the values at 50 K. These values of λ 's are adjusted to show a theoretical reproduction of the experimental data although they are quite a bit larger than those for SdH oscillation amplitudes. With the assumed λ 's, the calculated Hall coefficient is negative at high magnetic field and low temperature, becoming positive at high temperature (Fig. 3b), as in the experiment¹⁰.

The SdH oscillations are displayed in Fig. 3a by modifying the conductivity tensor σ_{ij} to include effects of the Landau levels³⁰. The above mentioned mean free paths (λ) are used for σ_{ij} itself; however, a reduction of λ 's by a factor of 0.05 is assumed for the modification factor of σ_{ij} for quantum oscillations, yielding SdH oscillation amplitudes close to experiments¹⁰. This may suggest that the quantum coherence is relaxed much faster than the classical linear momentum, but it is beyond the scope of our present work to justify the assumed λ 's. Nonetheless, our assumed λ of 20 nm at 1.5 K for SdH oscillations from the α and α' pockets is consistent with 17 nm from measured dHvA oscillations⁵. In our results, the low-frequency α and α' oscillations are much stronger than the high-frequency β oscillation since the average mean free *time* is larger for the holes than for the electrons even with the assumed λ 's because of the difference in their group velocities. Thus, the dominant oscillation in the Hall coefficient (Fig. 3a) originates from the hole pockets although the Hall coefficient itself is negative at high field due to the electron pocket.

Calculated SdH oscillations grow with the magnetic field (Fig. 3a), as in experiments¹⁰.

Compared with model calculations considering magnetic fluctuations^{11,12}, our results show that the presence of CuO chains in YBa₂Cu₃O_{6.5} is important for explaining the high-frequency quantum oscillation and the negative Hall coefficient. Since our results are based on a static long-range magnetic order stable in the LSDA+*U* method, fluctuations in real materials may modify the FS. As discussed above, one possibility is the evolution of the small-size hole pockets (α and α' in Fig. 1d) to arcs, as proposed by the model calculations.

While the *d*-density-wave theory predicts hole pockets larger than electron pockets, our result predicts an electron pocket larger than hole pockets, and assigns FS pockets to the observed frequencies oppositely. Thus, in our work, the observed major frequency originates from small-size hole pockets while the negative Hall coefficient is due to a large-size electron pocket.

For YBa₂Cu₄O₈, as in the case of YBa₂Cu₃O_{6.5}, we obtain very different FSs with and without AFM order in the CuO₂ planes (Fig. 4). With the LDA+*U* method with $U = 3.1$ eV and $J = 0.8$ eV for all Cu *d* orbitals, we obtain a FS consisting of large hole pockets and open orbits (Fig. 4b) which is consistent with previous first-principles calculations³¹. When the magnetic order is considered by the LSDA+*U* method with the same U and J , AFM order is stable in the CuO₂ planes with $0.22 \mu_B$ at each Cu atom, and the FS consists of small hole pockets (α and α' indicating the two largest ones), open orbits, and small electron pockets (β), as shown in Fig. 4d. The calculated FS pocket areas are 721 T (α), 729 T (α'), and 685 T (β), which are close to the measured value 660 T⁷, overestimating it by about 10 % or less. Contrary to YBa₂Cu₃O_{6.5}, the calculated FS pocket sizes in YBa₂Cu₄O₈ are sensitive to U and J around the used values. Calculated cyclotron effective masses, $0.45 m_e$ for holes and $0.52 m_e$ for electrons, are much smaller than the measured values of $2.7 \sim 3.0 m_e$ ⁷, but calculated Sommerfeld coefficient for the normal-state specific heat, $6.97 \text{ mJ}\cdot\text{mol}^{-1}\cdot\text{K}^{-2}$, is rather close to the experimental value of $9 \text{ mJ}\cdot\text{mol}^{-1}\cdot\text{K}^{-2}$ ³².

In summary, we have studied the electronic structures of YBa₂Cu₃O_{6.5} and YBa₂Cu₄O₈ by the LSDA+*U* method, and the results yield FS topologies fully consistent with quantum oscillation measurements. It is shown that the magnetic order in the CuO₂ planes may explain quantitatively the dHvA and SdH oscillation frequencies, the negative Hall coefficients, and the specific heat. These results point to the importance of magnetic order for understanding the electronic structures of the underdoped high- T_c cuprates.

This work was supported by the NRF of Korea (Grant Nos. KRF-2007-314-C00075, 2009-0081204, and 2011-0018306), by NSF under Grant No. DMR07-05941, and by the Director, Office of Science, Office of Basic Energy Sciences, Division of Materials Sciences and Engineering, U.S. DOE under Contract No. DE-AC02-05CH11231. Early version of LSDA+*U* methodology was supported by NSF; H.J.C. was supported by BES DMSE during collaborative visits. Computational resources have been provided by KISTI Supercomputing Center (Project No. KSC-2008-S02-0004), NSF through TeraGrid resources at SDSC, and DOE at LBNL's NERSC facility.

-
- * Email: h.j.choi@yonsei.ac.kr
- ¹ M. R. Norman, H. Ding, M. Randeria, J. C. Campuzano, T. Yokoya, T. Takeuchi, T. Takahashi, T. Mochiku, K. Kadowaki, P. Guptasarma, and D. G. Hinks, *Nature (London)* **392**, 157 (1998).
 - ² M. A. Hossain, J. D. F. Mottershead, D. Fournier, A. Bostwick, J. L. McChesney, E. Rotenberg, R. Liang, W. N. Hardy, G. A. Sawatzky, I. S. Elfimov, D. A. Bonn, and A. Damascelli, *Nat. Phys.* **4**, 527 (2008).
 - ³ N. Doiron-Leyraud, C. Proust, D. LeBoeuf, J. Levallois, J. Bonnemaïson, R. Liang, D. A. Bonn, W. N. Hardy, and L. Taillefer, *Nature (London)* **447**, 565 (2007).
 - ⁴ C. Jaudet, D. Vignolles, A. Audouard, J. Levallois, D. LeBoeuf, N. Doiron-Leyraud, B. Vignolle, M. Nardone, A. Zitouni, R. Liang, D. A. Bonn, W. N. Hardy, L. Taillefer, and C. Proust, *Phys. Rev. Lett.* **100**, 187005 (2008).
 - ⁵ S. E. Sebastian, N. Harrison, E. Palm, T. P. Murphy, C. H. Mielke, R. Liang, D. A. Bonn, W. N. Hardy, and G. G. Lonzarich, *Nature (London)* **454**, 200 (2008).
 - ⁶ A. Audouard, C. Jaudet, D. Vignolles, R. Liang, D. A. Bonn, W. N. Hardy, L. Taillefer, and C. Proust, *Phys. Rev. Lett.* **103**, 157003 (2009).
 - ⁷ A. F. Bangura, J. D. Fletcher, A. Carrington, J. Levallois, M. Nardone, B. Vignolle, P. J. Heard, N. Doiron-Leyraud, D. LeBoeuf, L. Taillefer, S. Adachi, C. Proust, and N. E. Hussey, *Phys. Rev. Lett.* **100**, 047004 (2008); E. A. Yelland, J. Singleton, C. H. Mielke, N. Harrison, F. F. Balakirev, B. Dabrowski, and J. R. Cooper, *ibid.* **100**, 047003 (2008).
 - ⁸ A. Carrington and E. A. Yelland, *Phys. Rev. B* **76**, 140508(R) (2007); I. S. Elfimov, G. A. Sawatzky, and A. Damascelli, *ibid.* **77**, 060504(R) (2008).
 - ⁹ D. Puggioni, A. Filippetti, and V. Fiorentini, *Phys. Rev. B* **79**, 064519 (2009).
 - ¹⁰ D. LeBoeuf, N. Doiron-Leyraud, J. Levallois, R. Daou, J.-B. Bonnemaïson, N. E. Hussey, L. Balicas, B. J. Ramshaw, R. Liang, D. A. Bonn, W. N. Hardy, S. Adachi, C. Proust, and L. Taillefer, *Nature (London)* **450**, 533 (2007).
 - ¹¹ N. Harrison, R. D. McDonald, and J. Singleton, *Phys. Rev. Lett.* **99**, 206406 (2007).
 - ¹² T. Morinari, arXiv:0805.1977.
 - ¹³ W. Chen, K. Yang, T. M. Rice, and F. C. Zhang, *Europhys. Lett.* **82**, 17004 (2008).
 - ¹⁴ S. Chakravarty and H.-Y. Kee, *PNAS* **105**, 8835 (2008); D. Podolsky and H.-Y. Kee, *Phys. Rev. B* **78**, 224516 (2008).
 - ¹⁵ J. Eun, X. Jia, and S. Chakravarty, *Phys. Rev. B* **82**, 094515 (2010).
 - ¹⁶ P. Wróbel, W. Suleja, and R. Eder, *Phys. Rev. B* **78**, 064501 (2008).
 - ¹⁷ A. J. Millis and M. R. Norman, *Phys. Rev. B* **76**, 220503(R) (2007).
 - ¹⁸ L. Onsager, *Phil. Mag.* **43**, 1006 (1952).
 - ¹⁹ P. Zhang, S. G. Louie, and M. L. Cohen, *Phys. Rev. Lett.* **98**, 067005 (2007).
 - ²⁰ D. Sánchez-Portal, P. Ordejón, E. Artacho, and J. M. Soler, *Int. J. Quantum Chem.* **65**, 453 (1997).
 - ²¹ A. I. Liechtenstein, V. I. Anisimov, and J. Zaanen, *Phys. Rev. B* **52**, R5467 (1995); S. Y. Park and H. J. Choi, *ibid.* **80**, 155122 (2009).
 - ²² J. Grybos, D. Hohlwein, Th. Zeiske, R. Sonntag, F. Kubanek, K. Eichhorn, and Th. Wolf, *Physica C* **220**, 138 (1994).
 - ²³ Y. Yamada, J. D. Jorgensen, S. Pei, P. Lightfoot, Y. Kodama, T. Matsumoto, and F. Izumi, *Physica C* **173**, 185 (1991).
 - ²⁴ E. Demler, S. Sachdev, and Y. Zhang, *Phys. Rev. Lett.* **87**, 067202 (2001).
 - ²⁵ D. Haug, V. Hinkov, A. Suchanek, D. S. Inosov, N. B. Christensen, Ch. Niedermayer, P. Bourges, Y. Sidis, J. T. Park, A. Ivanov, C. T. Lin, J. Mesot, and B. Keimer, *Phys. Rev. Lett.* **103**, 017001 (2009).
 - ²⁶ V. Hinkov, D. Haug, B. Fauqué, P. Bourges, Y. Sidis, A. Ivanov, C. Bernhard, C. T. Lin, and B. Keimer, *Science* **319**, 597 (2008); A. P. Kampf, *Phys. Rep.* **249**, 219 (1994); R. J. Birgeneau, C. Stock, J. M. Tranquada, and K. Yamada, *J. Phys. Soc. Jpn.* **75**, 111003 (2006); S. M. Hayden, G. Aeppli, H. Mook, D. Rytz, M. F. Hundley, and Z. Fisk, *Phys. Rev. Lett.* **66**, 821 (1991); B. Lake, G. Aeppli, K. N. Clausen, D. F. McMorrow, K. Lefmann, N. E. Hussey, N. Mangkorntong, M. Nohara, H. Takagi, T. E. Mason, and A. Schröder, *Science* **291**, 1759 (2001).
 - ²⁷ Y. Ando, K. Segawa, S. Komiyama, and A. N. Lavrov, *Phys. Rev. Lett.* **88**, 137005 (2002).
 - ²⁸ D. Haug, V. Hinkov, Y. Sidis, P. Bourges, N. B. Christensen, A. Ivanov, T. Keller, C. T. Lin, and B. Keimer, *New J. Phys.* **12**, 105006 (2010); S. E. Sebastian, N. Harrison, M. M. Altarawneh, C. H. Mielke, R. Liang, D. A. Bonn, W. N. Hardy, and G. G. Lonzarich, *Proc. Nat. Am. Soc.* **107**, 6175 (2010); J. Singleton, C. de la Cruz, R. D. McDonald, S. Li, M. Altarawneh, P. Goddard, I. Franke, D. Rickel, C. H. Mielke, X. Yao, and P. Dai, *Phys. Rev. Lett.* **104**, 086403 (2010).
 - ²⁹ J. W. Loram, J. Luo, J. R. Cooper, W. Y. Liang, and J. L. Tallon, *J. Phys. Chem. Solids* **62**, 59 (2001).
 - ³⁰ T. Ando, *J. Phys. Soc. Jpn.* **37**, 1233 (1974).
 - ³¹ J. Yu, K. T. Park, and A. J. Freeman, *Physica C* **172**, 467 (1991).
 - ³² J.W. Loram, APS March Meeting, Denver, Colorado.
 - ³³ S. E. Sebastian, N. Harrison, P. A. Goddard, M. M. Altarawneh, C. H. Mielke, R. Liang, D. A. Bonn, W. N. Hardy, O. K. Andersen, and G. G. Lonzarich, *Phys. Rev. B* **81**, 214524 (2010).

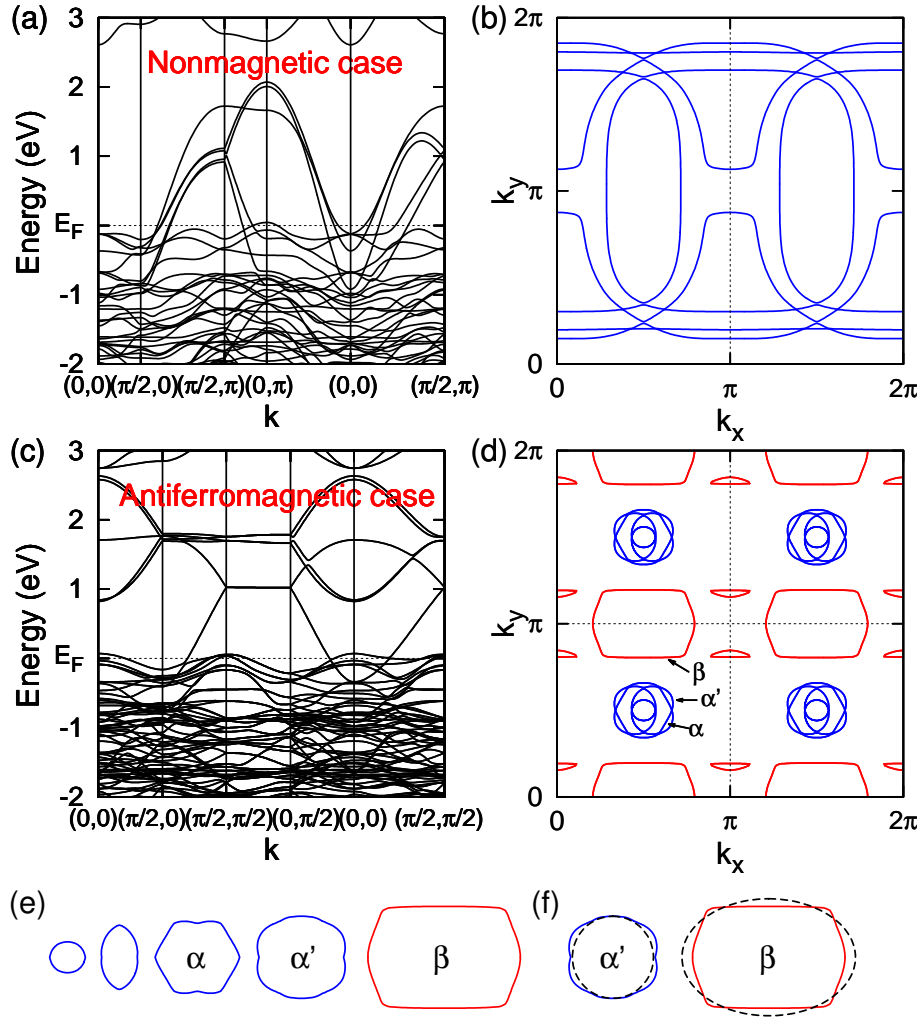


FIG. 1: (Color online) Electronic structures in ortho-II $\text{YBa}_2\text{Cu}_3\text{O}_{6.5}$ with Coulomb interaction at Cu d orbitals ($U = 6.0$ eV and $J = 1.0$ eV). (a) The band structure and (b) the FS obtained by the LDA+ U method with no magnetic order. (c) The band structure and (d) the FS obtained by the LSDA+ U method with (π, π) AFM order in the CuO_2 planes. In (b) and (d), the FSs are drawn in the Brillouin zone of a real-space unit cell (0.383×0.387 nm²) containing a Cu atom on each CuO_2 plane. Blue (red) lines are hole pockets and open orbits (electron pockets). (e) FS pockets in (d). The α , α' , and β pocket areas are 485, 621, and 1450 T, respectively. The shape of the α' pocket is close to the rounded square reported by the angle-dependent quantum oscillation measurement³³. (f) Comparison with experimental FS pocket areas (630 T⁶ and 1650 T⁵) in dashed lines. A FS area of 1 nm⁻² corresponds to a frequency of 105 T¹⁸.

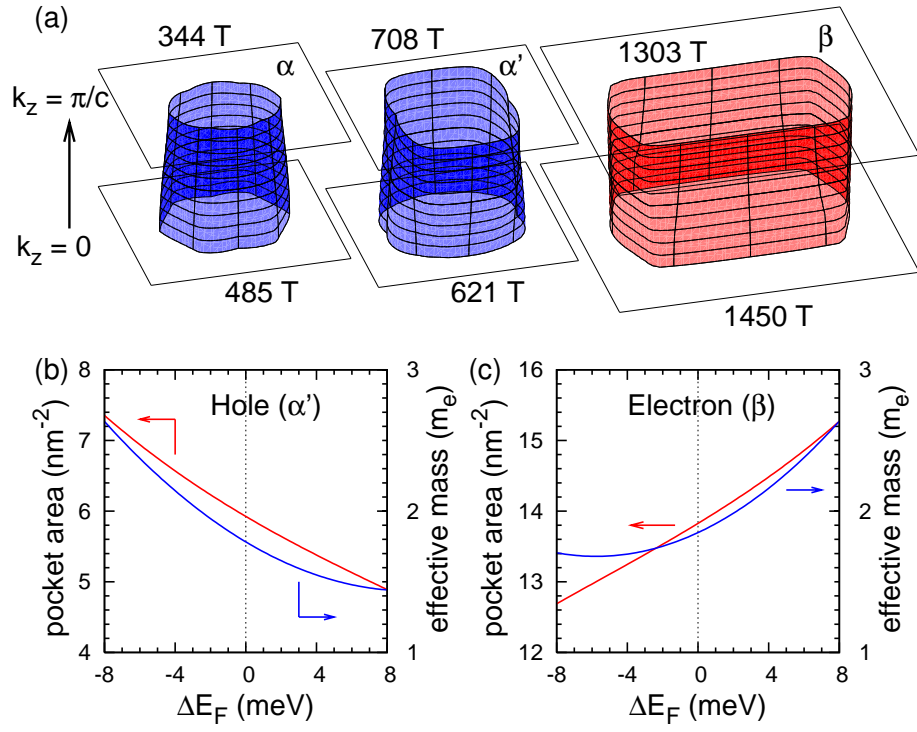


FIG. 2: (Color online) FS pocket sizes versus k_z and cyclotron effective masses in $\text{YBa}_2\text{Cu}_3\text{O}_{6.5}$. (a) FS pocket areas perpendicular to the k_z -axis when the Fermi level is at the charge-neutrality level. (b) Hole and (c) electron pocket areas and their cyclotron effective masses as functions of the Fermi-level shift (ΔE_F) from the charge-neutrality level. The indexes α , α' , and β are the same as in Fig. 2d. A FS area of 1 nm^{-2} corresponds to a frequency of 105 T^{18} .

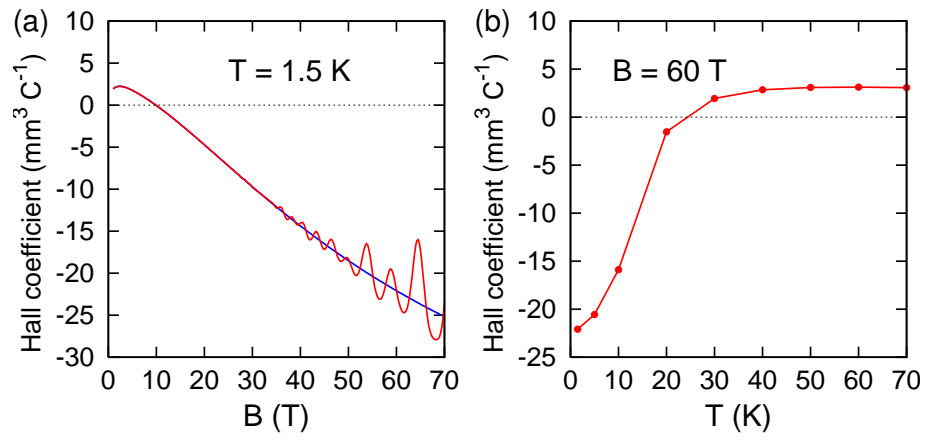


FIG. 3: (Color online) Hall coefficients for YBa₂Cu₃O_{6.5}. (a) Hall coefficient versus magnetic field (B) at temperature $T = 1.5$ K, with and without the SdH oscillation (red and blue lines, respectively). (b) Hall coefficient versus temperature at $B = 60$ T without considering the SdH oscillation.

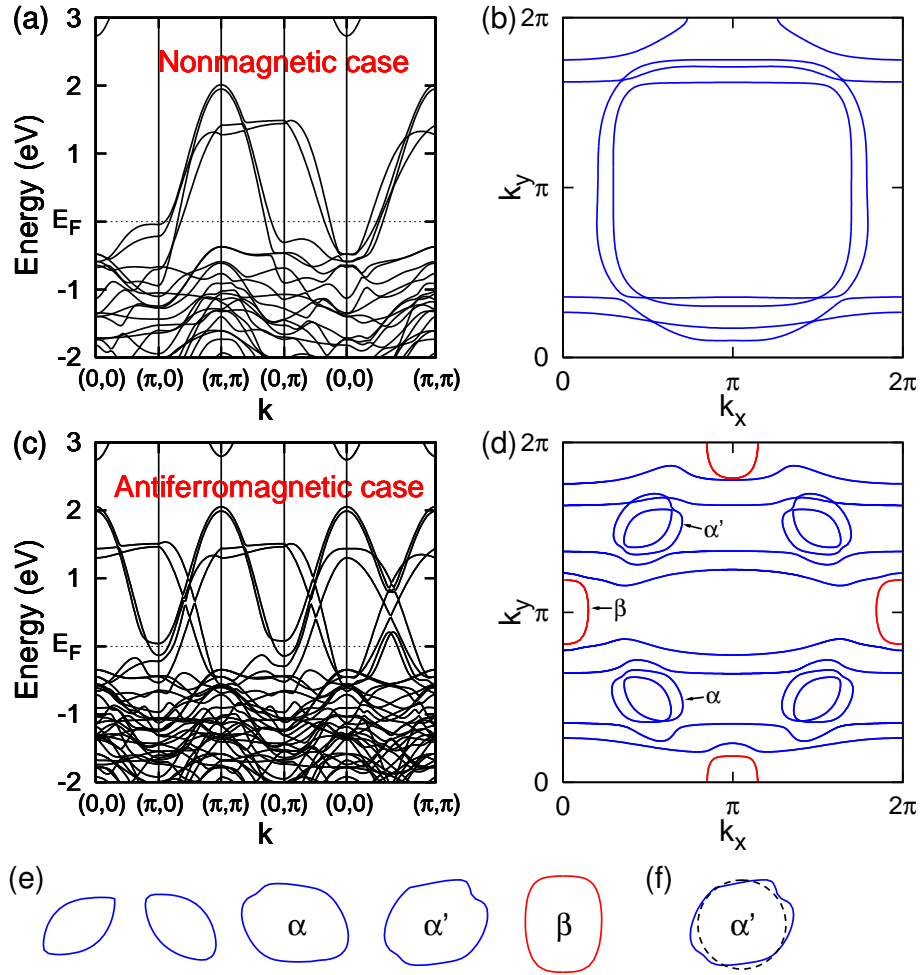


FIG. 4: (Color online) Electronic structures in $\text{YBa}_2\text{Cu}_4\text{O}_8$ with Coulomb interaction at Cu d orbitals ($U = 3.1$ eV and $J = 0.8$ eV). (a) The LDA+ U band structure and (b) the FS in the non-magnetic case. (c) The LSDA+ U band structure and (d) the FS with (π, π) AFM order in the CuO_2 planes. In (b) and (d), the FSs are drawn in the Brillouin zone of a real-space unit cell (0.384×0.387 nm 2) containing a Cu atom on each CuO_2 plane. Blue (red) lines are hole pockets and open orbits (electron pockets). (e) FS pockets in (d). The α , α' , and β pocket areas are 721, 729, and 685 T, respectively. (f) Comparison with the measured FS pocket area (660 T 2) in the dashed line.